

Comparative Study of Different Control Algorithms on Brushless DC Motors

B. Pavan Kumar

P.G scholar, Dept. of EEE

Amrita School of Engineering, Bangalore, India

Amrita Vishwa Vidyapeetham

bolugamrohan@gmail.com

Krishnan C.M.C

SG, Dept. of EEE

Amrita School of Engineering, Bangalore, India

Amrita Vishwa Vidyapeetham

cmckrishnan@gmail.com

Abstract— Recently, the role of a BLDC (Brushless Direct Current) motor is favoring the designers due to its higher efficiency. Most of the applications are already using BLDC motors as a replacement for AC motors and this holds true for innumerable applications, and these motors also reduce the overall system weight. The commutation of BLDC motor is done electronically; hence it is quite simple to control the torque and RPM of the motor even at much higher speed. This paper gives a brief comparative study of three different control schemes i.e Sinusoidal field oriented control (FOC), Field oriented control (FOC), Hysteresis control of a BLDC motor primarily on the aspect of output torque ripple. The study of all the three control schemes is discussed briefly and simulation of control algorithm has been performed.

Index Terms—Brushless DCMotor (BLDC), Field Oriented Control (FOC), Electro Motive Force(EMF).

I. INTRODUCTION

BLDC MOTORS are increasingly being used in many application fields like industrial automation, electric vehicles, aircraft, machine tools, computer, numerical control machines and robotics due to the simplicity in the control scheme, reliability, maintenance free operation, high efficiency and high torque/inertia ratio. In all of these applications, achievement of ripple free torque is the major concern, merely due to the uncertainties, parameter variations, harmonics, etc., an efficient control mechanism is required which is robust enough to overcome these effects present in the system [10].

The machine design and control techniques are used to reduce the torque ripple. The three major sources for torque production in BLDCM's are listed as below. Firstly cogging torque is caused due to the interaction between stator slots and rotor magnetic field, which is independent of stator current excitation. Secondly, reluctance torque is due to variation of phase inductance with respect to position. Lastly mutual torque is due to coupling between stator winding current and rotor magnetic field. As the cogging torque and reluctance torque are highly

influenced by the machine design, the effect of these can be greatly scaled down by designing BLDCM with low saliency by one slot pitch.

In recent years, a study has been done in identifying the sources for minimization of torque ripples in BLDCM's. An auto-tuning method using repetitive control parameter for reduction of mechanical vibration and acoustic noise caused by structural imperfections is discussed in [1]. As the six step commutation torque ripple results in spikes and dips in low and high speed ranges, much research regarding the commutation torque ripple has been done in [2]. Phase voltage control by adjusting the duty ratio during commutation intervals is discussed in [3]. The delay of the switch off point of outgoing switch using overlap switching method has been introduced in [4]. The methods which deal with the cancellation of the harmonics generally require the machine parameters which are undesirable if the operating point changes discussed in [5]. A current control strategy with an adaptive internal model is proposed in [6]. A passive filter is used in [7] to reduce the torque ripples. To overcome such difficulty, an active filter is used to reduce the torque ripple in [8], but this result in much higher cost of the implementation.

Most of the literature survey has assumptions like three phases generate identical back EMF waveforms and excitation of motor exhibit half wave symmetry which might not be reliable in practice. The method discussed in this paper makes no such assumptions, where the natural a-b-c reference frame is transformed to the d-q-o reference frame. The operation of the method is compared against other methods in terms of torque ripple minimization and maximization of the mutual torque component. The comparative study of three different control schemes is discussed in detail and simulation study of all three control schemes is performed. The sinusoidal FOC control scheme gives less torque ripple out of all the control schemes which is demonstrated by a simulation study in the paper.

II. TRAPEZOIDAL BACK EMF MACHINE MODEL

The equation in the abc reference frame can be written in the following form

$$\overrightarrow{v_{abcs}} = r\overrightarrow{i_{abcs}} + L \frac{d}{dt} \overrightarrow{i_{abcs}} + w_r \overrightarrow{\lambda_{abcs}} \quad (1)$$

The non-sinusoidal back EMF and non-sinusoidal instantaneous currents are given as [9].

$$e_a = E_m \cos(\theta_r + \mu) \quad (2)$$

$$e_b = E_m \cos\left(\theta_r + \mu - \frac{2\pi}{3}\right) \quad (3)$$

$$e_c = E_m \cos\left(\theta_r + \mu + \frac{2\pi}{3}\right) \quad (4)$$

$$i_a = \frac{1}{\epsilon} E_m \cos(\theta_r + \mu) \quad (5)$$

$$i_b = \frac{1}{\epsilon} E_m \cos\left(\theta_r + \mu - \frac{2\pi}{3}\right) \quad (6)$$

$$i_c = \frac{1}{\epsilon} E_m \cos\left(\theta_r + \mu + \frac{2\pi}{3}\right), \quad (7)$$

where, e_a , e_b , e_c are the phase back EMF voltage for phase a, b and c respectively [9].

$$\mu(\theta_r) = a \tan\left(\frac{-\lambda_q s}{\lambda_d s}\right) - \theta_r \quad (8)$$

$$= \sqrt{(\lambda_q s^2 + \lambda_d s^2)} / \lambda_m \quad (9)$$

Here μ and ϵ are periodic variables in normalized form and are functions of rotor position.

The output power of the machine is

$$P_{out} = [e_a i_a + e_b i_b + e_c i_c] \quad (10)$$

$$P_{out} = \frac{3}{2} E_m I_m \quad (11)$$

The equation for torque using peak flux linkage and peak currents is given below [9].

$$T_e = \frac{3}{2} \frac{P}{2} \lambda_m I_m \quad (12)$$

Since all the variables in the equation (12) above are constant in time, it proves that the solution obtained from non-sinusoidal currents generate ripple free torque.

III. IMPLEMENTATION OF FIELD ORIENTED CONTROL

Step 1:

The two phases of the 3-phase stator currents are measured and the third phase i_c is calculated from the relationship given below:

$$i_a + i_b + i_c = 0 \quad (13)$$

Step 2:

The conversion of 3-phase currents to a two axis system is given using Clark's transformation as below.

Clark's Transformation:

$$i_\alpha = i_a \quad (14)$$

$$i_\beta = (i_a + 2i_b)/\sqrt{3} \quad (15)$$

Here the transformed currents are time-varying values as viewed from the stator perspective.

Step 3:

The two axis coordinate system which is generated in step 2 is then transformed so as to align with the rotor magnetic flux. This conversion is known as the Park's transformation.

The Park's transformation is given as:

$$I_d = i_\alpha \cos \theta + i_\beta \sin \theta \quad (16)$$

$$I_q = -i_\alpha \sin \theta + i_\beta \cos \theta \quad (17)$$

Step 4:

The reference values for I_d is generally kept zero for a permanent magnet motor whereas the I_q reference is generated from the torque command generated from the speed loop. These two values are compared with the actual feedback from the motor which generates error inputs for the two PI controllers. The output from the controllers provides voltages vectors V_d and V_q .

Step 5:

The V_d and V_q voltages from the controller are translated back to the stationary reference frame using inverse park's transformation.

Inverse park's transformation is given as:

$$V_\alpha = V_d \cos \theta - V_q \sin \theta \quad (18)$$

$$V_\beta = V_d \sin \theta + V_q \cos \theta \quad (19)$$

Step 6:

The V_α and V_β values are transformed back to the 3-phase quantities V_a , V_b and V_c .

Inverse Clark's transformation is given as:

$$V_a = V_\beta \quad (20)$$

$$V_b = (-V_\beta + \sqrt{3}V_\alpha)/2 \quad (21)$$

$$V_c = (-V_\beta - \sqrt{3}V_\alpha)/2 \quad (22)$$

The resulting voltage signals V_a , V_b and V_c are then used to perform the pulse width modulation. It is the reference frame transformations that serve the work of converting between the sinusoidal time variant current and voltage signals at the motor windings into the DC signal representations in the d-q space.

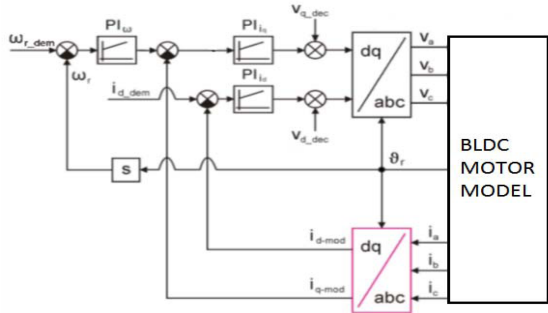


Fig. 1. Block diagram of field oriented control.

IV. SINUSOIDAL INJECTION SCHEME CONTROL FOR FOC

The corresponding rotor reference frame model is

$$\begin{bmatrix} v_{ds}^r \\ v_{qs}^r \end{bmatrix} = \begin{bmatrix} r_s + w_r L_s \frac{1}{K} \frac{dK}{d\theta_r} & w_r L_s \left(1 + \frac{d\mu}{d\theta_r}\right) \\ -w_r L_s \left(1 + \frac{d\mu}{d\theta_r}\right) & r_s + w_r L_s \frac{1}{K} \frac{dK}{d\theta_r} \end{bmatrix} \begin{bmatrix} i_{ds}^r \\ i_{qs}^r \end{bmatrix} + \begin{bmatrix} L_s & 0 \\ 0 & L_s \end{bmatrix} \frac{d}{dt} \begin{bmatrix} i_{ds}^r \\ i_{qs}^r \end{bmatrix} + w_r \lambda_m \begin{bmatrix} 0 \\ \frac{1}{K^2} \end{bmatrix} \quad (23)$$

When $k=1$ and $\mu=0$, the model takes the form of sinusoidal control while the decoupling terms are expressed as

$$\begin{bmatrix} v_{ds}^r \\ v_{qs}^r \end{bmatrix} = \begin{bmatrix} w_r L_s \frac{1}{k} \frac{dK}{d\theta_r} & w_r L_s \left(1 + \frac{d\mu}{d\theta_r}\right) \\ -w_r L_s \left(1 + \frac{d\mu}{d\theta_r}\right) & w_r L_s \frac{1}{K} \frac{dK}{d\theta_r} \end{bmatrix} \begin{bmatrix} i_{ds}^r \\ i_{qs}^r \end{bmatrix} + w_r \lambda_m \begin{bmatrix} 0 \\ \frac{1}{K^2} \end{bmatrix} \quad (24)$$

V. SIMULATION RESULTS

Simulation is carried out for the MATLAB model with parameters is shown in Table.1 shown below

TABLE I. MOTOR PARAMETERS.

Power rating (Watts)	400 Watts
Inverter input (DC)	120 Volts
Stator resistance (R_s)	2.8750 Ω
Stator inductance (L_s)	$8.5e^{-3}$ H
Torque constant	1.4 N.m
Flux linkage (λ_m)	0.175 V.s
Moment of inertia	0.0008 Kg. m ²
Pole pairs	4

Simulation is carried out for all the three control schemes, firstly open loop simulation is executed for the simulation model of the BLDC motor which is expressed in the Fig. 2 and Fig. 3. Here Fig. 1 shows one of the phase waveforms of hall sensor, stator currents and stator back EMF's.

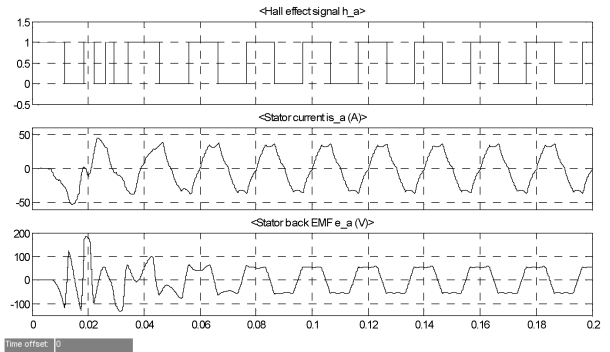


Fig. 2. Waveforms of A phase of the motor (a) Hall effect sensor (b) stator current (c) stator back EMF's

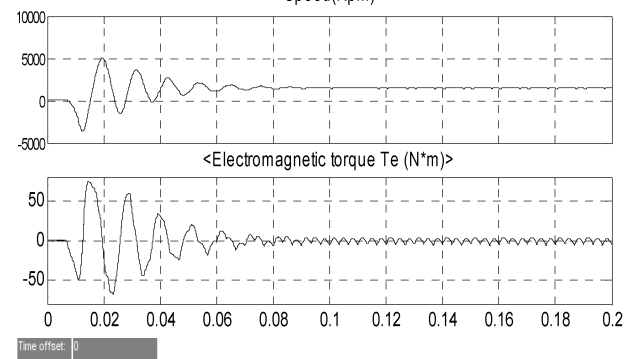


Fig. 3. (a) Speed (b) Electromagnetic Torque (open-loop).

Fig. 4 shows the magnified waveform of the above figure where there is a significant ripple in torque at no load condition which is the major issued solved by the control schemes which are discussed later in the paper.

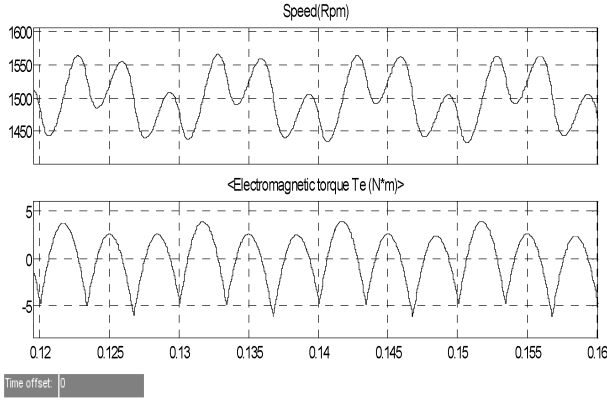


Fig. 4. (a) Speed (b) Electromagnetic Torque (open-loop).

The above open loop simulation is done at N=1400 Rpm and torque applied is 15 N-m which shown in Fig. 3 and Fig. 4. Below Fig. 5 shows the stator phase currents for the open loop simulation of the motor.

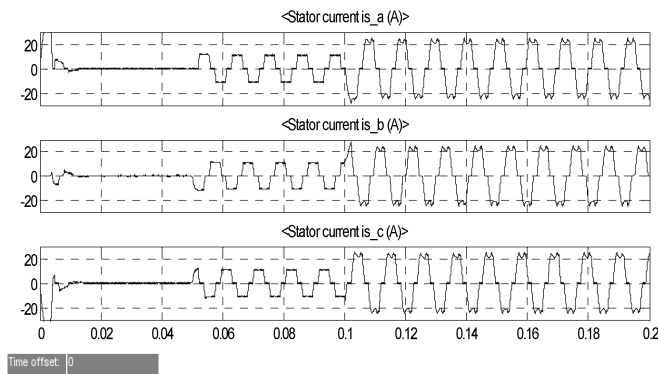


Fig. 5. Waveforms of phase stator currents (open-loop).

Referable to the drawbacks in the open loop simulation three different control system simulation is performed to surmount the problem of torque ripple. Below are the results obtained by the hysteresis control for the same motor which is simulated with the MATLAB model of the motor.

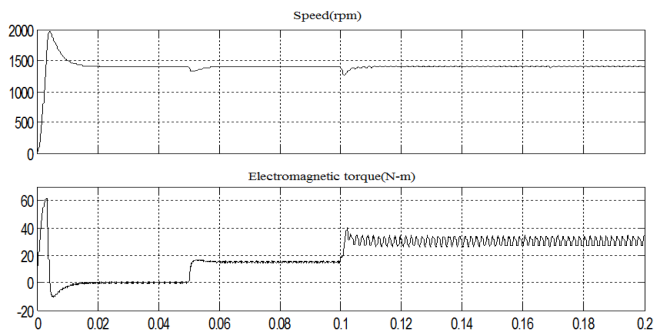


Fig. 6. (a) Speed (b) Electromagnetic Torque (hysteresis control).

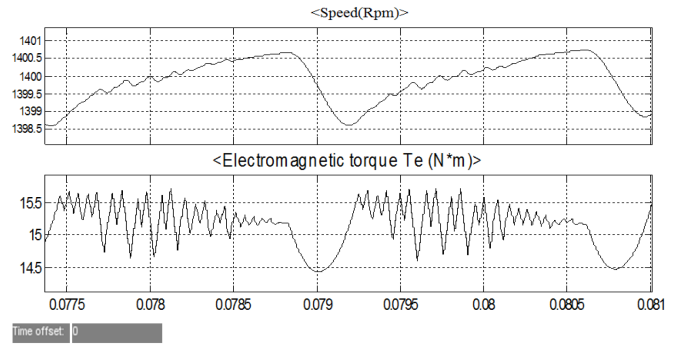


Fig. 7. (a) Speed (b) Electromagnetic Torque (hysteresis control).

The electromagnetic torque ripple in open loop simulation and hysteresis control are as shown in Figs. 3 to 7 and a greater reduction in torque ripple is seen with the hysteresis control. Hysteresis control has a problem with the selection of appropriate hysteresis band. Additionally since the control is in a-b-c frame, the tuning of PI is difficult at higher speeds due to its low-pass effect. This problem can be solved by keeping PI controller in dq framework as done in FOC. This is also shown in the simulation in Fig. 9 and Fig. 10.

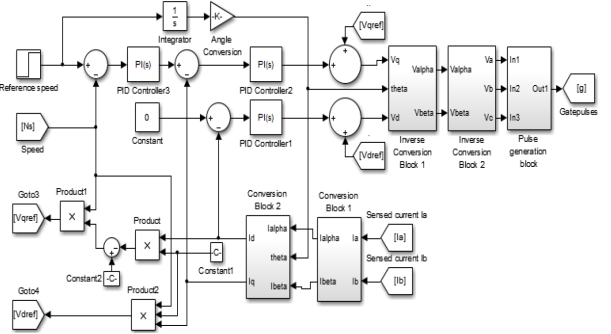


Fig. 8. Block diagram of Sinusoidal FOC scheme.

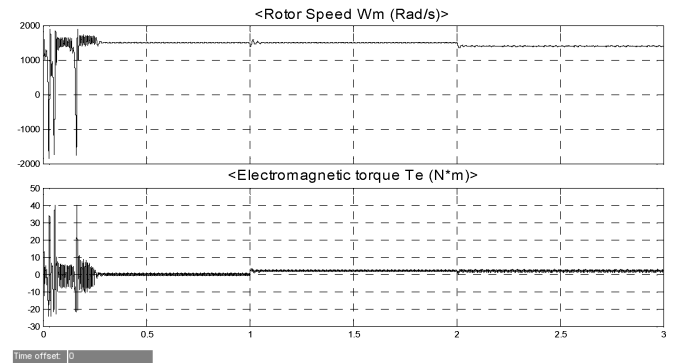


Fig. 9. (a) Speed (b) Electromagnetic Torque (FOC).

By using FOC, there is a greater reduction in torque ripple, but the control scheme has huge transient dynamics which is shown

in Fig. 9 above. This problem can be tackled by using sinusoidal FOC schemes as clearly seen in Figs. 11 and 12.

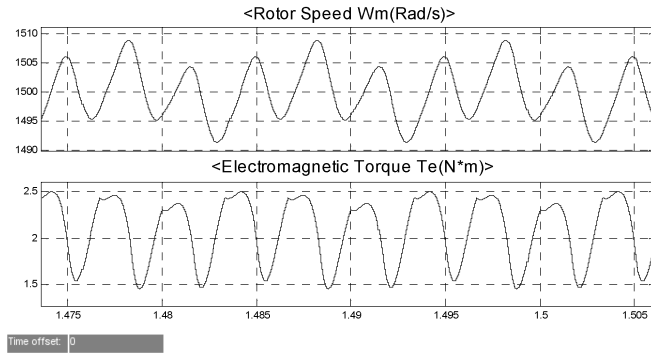


Fig. 10. (a) Speed (b) Electromagnetic Torque (FOC).

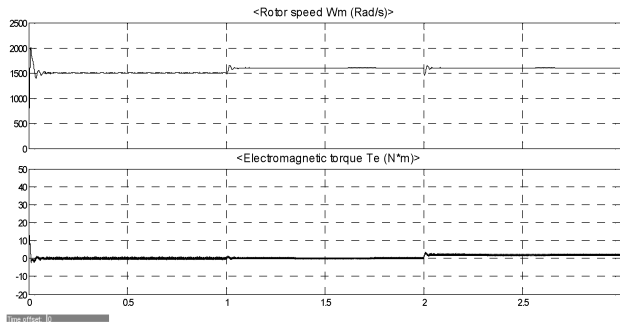


Fig. 11. (a) Speed (b) Electromagnetic Torque (sinusoidal FOC).

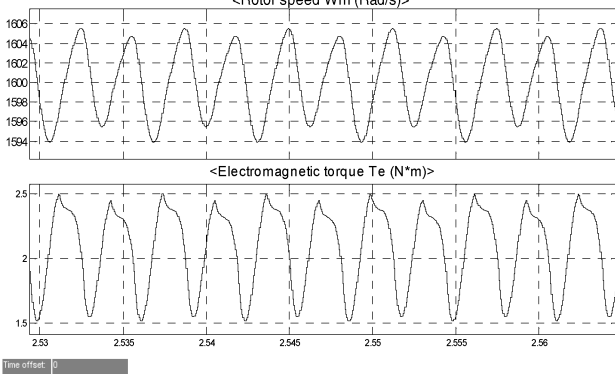


Fig. 12. (a) Speed (b) Electromagnetic Torque (sinusoidal FOC).

VI. CONCLUSIONS

The three different control schemes are analyzed for the BLDC motor and a comparative study is performed on the aspect of ripple free torque operation. All the simulations are done with motor model in MATLAB Simulink software. Out of the three control schemes, sinusoidal FOC is performing better in terms of reduction in torque ripple as shown in the simulations.

REFERENCES

- [1] Hattori, Satomi, Muneaki Ishida, and Takamasa Hori. "Suppression control method for torque vibration of brushless dc motor utilizing repetitive control with fourier transform." In Proceedings. 6th International Workshop on Advanced Motion Control, pp. 427-432, 2000.
- [2] Won, Chang-hee, Joong-Ho Song, and Ick Choy. "Commutation torque ripple reduction in brushless DC motor drives using a single DC current sensor." In IEEE 33rd Annual Power Electronics Specialists Conference, vol. 2, pp: 985-990, 2002.
- [3] Cros, J., J-M. Vinassa, S. Clenet, S. Astier, and M. Lajoie-Mazenc. "A novel current control strategy in trapezoidal EMF actuators to minimize torque ripples due to phases commutations." In IET Fifth European Conference on Power Electronics and Applications, pp: 266-271, 1993.
- [4] Murai, Yoshihiro, Yoshihiro Kawase, Kazuharu Ohashi, Kazuo Nagatake, and Kyugo Okuyama. "Torque ripple improvement for brushless DC miniature motors." IEEE Transactions on Industry Applications, vol. 25, no. 3, pp: 441-450, 1989.
- [5] J. Holz and L. Springob, "Identification and compensation of torque ripple in high-precision permanent magnet motor drives," IEEE Trans. Ind. Electron., vol. 43, pp. 309-320, 1996.
- [6] Vladan Petrovic, Romeo Ortega, Aleksandar M. Stankovic', and Gilead Tadmor, "Design and Implementation of an Adaptive Controller for Torque Ripple Minimization in PM Synchronous Motors," IEEE Transactions on Power Electronics, vol. 15, no. 5, pp. 871-880, 2000.
- [7] K. Gulez, A.A. Adam, I.E. Buzcu, H. Pastaci, "Using passive filters to minimize torque pulsations and noises in surface PMSM derived field oriented control," Simulation Modeling Practice and Theory, pp: 989–1001 15th August 2007.
- [8] K. Gulez, A.A. Adam, Reduction of torque pulsation and noises in PMSM with hybrid filter topology," Simulation Modeling Practice and Theory, pp:350–361, 19th August, 2011.
- [9] Kshirsagar, Parag, and R. Krishnan. "High-efficiency current excitation strategy for variable-speed nonsinusoidal back-emf pmsm machines." IEEE Transactions on Industry Applications, vol. 48, no. 6, pp: 1875-1889, 2012.
- [10] J. U. Duncombe, "Infrared navigation—Part I: An assessment of feasibility," IEEE Trans. Electron Devices, vol. ED-11, no. 1, pp. 34–39, Jan. 1959.
- [11] Cho, Kwan-Yuhl, Yong-Kyun Lee, Hyungssoo Mok, Hag-Wone Kim, Byoung-Ho Jun, and Younghoon Cho. "Torque Ripple Reduction of a PM Synchronous Motor for Electric Power Steering using a Low Resolution Position Sensor." Journal of Power Electronics, vol. 10, no. 6, pp: 709-716, 2010.
- [12] Kim, Dae-Kyong, Kwang-Woon Lee, and Byung-II Kwon. "Commutation torque ripple reduction in a position sensorless brushless DC motor drive." IEEE Transactions on Power Electronics, vol.21, no. 6, pp: 1762-1768, 2006.